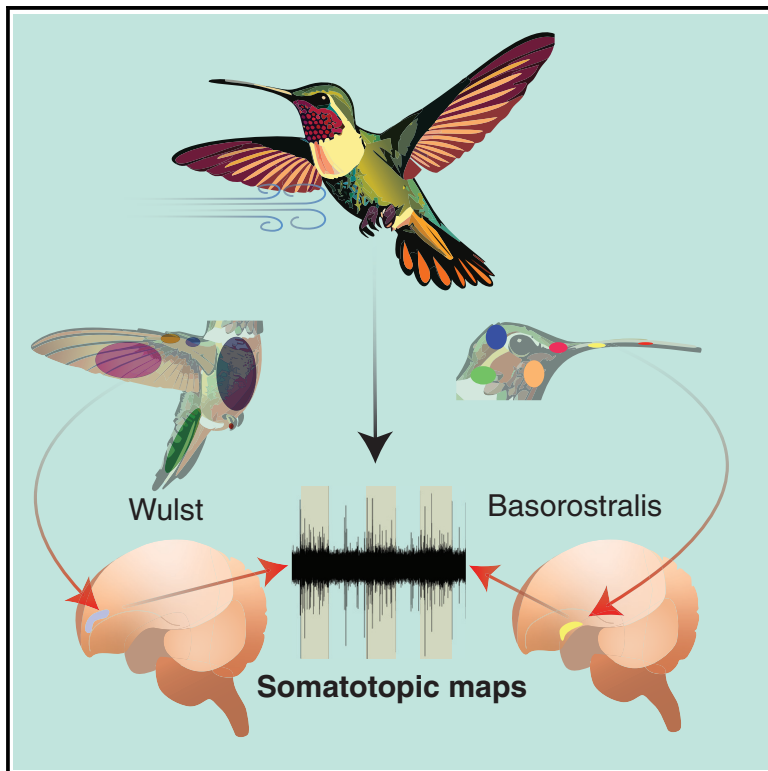


Current Biology

Variations in touch representation in the hummingbird and zebra finch forebrain

Graphical abstract



Authors

Andrea H. Gaede, Pei-Hsuan Wu,
Duncan B. Leitch

Correspondence

agaede@rvc.ac.uk (A.H.G.),
dleitch@ucla.edu (D.B.L.)

In brief

Using *in vivo* electrophysiology in hummingbirds and zebra finches, Gaede et al. reveal 3-dimensional maps of the body within two discrete nuclei of the forebrain. These new data also show that feathers of the leading edge of the wing and from the skin of the hindlimb are acutely sensitive to force, including air puffs associated with flight.

Highlights

- Somatosensation provides critical information for behaviors necessary for survival
- Hummingbird and finch forebrain cells respond to fine tactile stimuli such as airflow
- Both species show distinct body and head representations in separate forebrain areas
- Found continuous somatotopic maps with prominent representations of wing/foot



Report

Variations in touch representation in the hummingbird and zebra finch forebrain

Andrea H. Gaede,^{1,*} Pei-Hsuan Wu,² and Duncan B. Leitch^{2,3,4,*}¹Structure and Motion Laboratory, Department of Comparative Biomedical Sciences, Royal Veterinary College, 4 Royal College Street, London NW1 0TU, UK²Department of Zoology, University of British Columbia, #3051 - 6270 University Blvd. Vancouver, BC V6T 1Z4, Canada³Department of Integrative Biology & Physiology, University of California, Los Angeles, 621 Charles E. Young Drive South, Los Angeles, CA 90095, USA⁴Lead contact*Correspondence: agaede@rvc.ac.uk (A.H.G.), dleitch@ucla.edu (D.B.L.)<https://doi.org/10.1016/j.cub.2024.04.081>

SUMMARY

Somatosensation is essential for animals to perceive the external world through touch, allowing them to detect physical contact, temperature, pain, and body position. Studies on rodent vibrissae have highlighted the organization and processing in mammalian somatosensory pathways.^{1,2} Comparative research across vertebrates is vital for understanding evolutionary influences and ecological specialization on somatosensory systems. Birds, with their diverse morphologies, sensory abilities, and behaviors, serve as ideal models for investigating the evolution of somatosensation. Prior studies have uncovered tactile-responsive areas within the avian telencephalon, particularly in pigeons,^{3–6} parrots,⁷ and finches,⁸ but variations in somatosensory maps and responses across avian species are not fully understood. This study aims to explore somatotopic organization and neural coding in the telencephalon of Anna's hummingbirds (*Calypte anna*) and zebra finches (*Taeniopygia guttata*) by using *in vivo* extracellular electrophysiology to record activity in response to controlled tactile stimuli on various body regions. These findings reveal unique representations of body regions across distinct forebrain somatosensory nuclei, indicating significant differences in the extent of areas dedicated to certain body surfaces, which may correlate with their behavioral importance.

RESULTS

Hummingbirds are specialist nectarivores with unique demands on tactile sensation for precision hovering and feeding (Figure 1A). Their sensory systems are tuned for fast control of flight and specialized tongue movements.^{9–13} In contrast, songbirds like finches use a flap-bounding flight style and employ their bills for foraging and manipulation (Figure 1B).

Mechanoreceptor structures are associated with feathers of the wing and skin.

We hypothesized that feathers of the wing, including those associated with filoplume and leading-edge feathers, would show innervation by mechanosensory end organs. Herbst corpuscles (avian-specific homologs of Pacinian lamellated corpuscles) have been associated with the non-feathered skin of the beak in ducks,¹⁴ kiwis,¹⁵ and shore-foraging birds^{16,17} that localize prey using vibration detection via specialized sensory pits at the rostral margins of the beak. Along feather-covered surfaces, Herbst corpuscles are associated with the follicles of facial bristle feathers,¹⁸ conspicuous whisker-like feathers that appear from margins of the mouth and above the eyes in diverse lineages of birds including kiwis¹⁹ and owls.²⁰

We performed anterograde tracing in the wings of 4 hummingbirds, applying the lipophilic dye Dil (1,1'-dioctadecyl-3,3,3',3'-tetramethylindocarbocyanine) to the proximal ends of cut nerves of the brachial plexus including the radial nerve

(Figure 1C). At the wing's leading edge, primary and filoplume feather follicles are innervated by a ring-like "arcade" network²¹ of large, myelinated fibers (Figure 1D). Finer, unmyelinated, free nerve endings extend to more superficial layers of the epidermis.

We next analyzed how mechanoreceptors are distributed across the leading edge. *In vivo* subcutaneous injections of fluorescent AM1-43, followed by anterior to posterior tactile stimulation (mimicking air flow patterns during flight) were used to visualize locations of sensory neurons. Distinct swellings associated with putative Herbst corpuscles were sparse but enriched adjacent to feather follicle complexes (Figure 1E). These structures were similar in diameter to Herbst corpuscles observed in other avian taxa (Figure S1).^{22–29} This conformation suggests that these Pacinian corpuscles homologs are potentially well-positioned to detect mechanical deflection associated with diverse flight.

Rostral Wulst central organization

Visually responsive areas of the hyperpallium (Wulst) receive input via the thalamofugal system, whereas the somatosensory rostra Wulst (rWulst) is the destination of ascending fibers from a dorsal thalamic nucleus (nucleus dorsalis intermedialis ventralis anterior, DIVA).^{30,31} DIVA is targeted by the dorsal column nuclei.³²

In both species, we identified receptive fields corresponding to mechanical stimulation of the contralateral non-facial body.



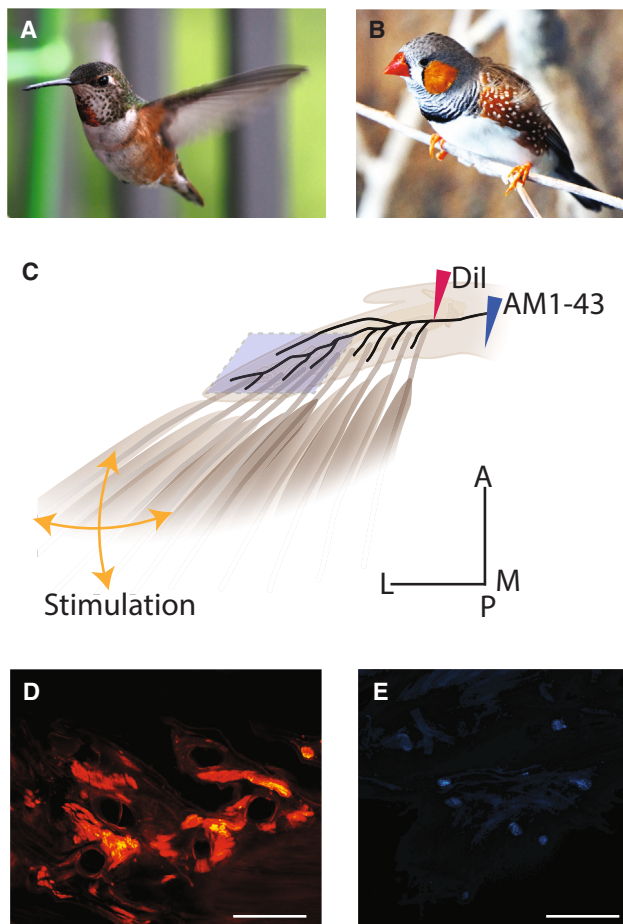


Figure 1. Comparative anatomy of avian tactile systems

(A) Hummingbirds have sensory adaptations (e.g., optic flow analysis) facilitating hovering flight. Photo by authors.

(B) Zebra finches employ intermittent flight while foraging. Photo used under a Creative Commons license.

(C) Experimental preparation for visualizing innervation to feathered wing surface. In hummingbirds, AM1-43 was injected into the subcutaneous space between the wing and dorsal surface (arrowhead), followed by 1 h of brushing of wing feathers in various directions. AM1-43 distribution was observed near the base of the feathers of the wing (shaded polygon). In other hummingbirds, Dil was applied to the proximal branch of the radial nerve innervating the wing, followed by > 1 month of passive transport to distal margins.

(D) Dil labeling shows the arcade of myelinated fibers at the feather/dermis juncture. Scale = 1 mm.

(E) Putative mechanosensory Herbst corpuscles labeled with AM1-43 in a hummingbird wing, following mechanical stimulation. Scale = 1 mm. See also Figure S1.

The rWulst includes the most superficial lamina of Wulst (hyperpallium apicale, HA; located medially at rostral levels), then ventrolaterally the narrow somatosensory thalamo-recipient lamina called the interstitial nucleus of hyperpallium apicale (IHA), and finally the dorsal mesopallium (M) more laterally^{33,34} (Figures 2A and 2B). Tactile responses, extending from the upper back/nape to the tail feathers and hindlimb, were marked on photographs following repeated manual stimulation.

Moving the electrode deeper, we found a progression in body representation. For example, in one finch rWulst recording track,

receptive fields gradually progressed from the upper back/nape (3100 μm depth) to the shoulder/wing (3300 μm), to mid back (3500 μm), and finally to tail feathers (3700 μm) (Figure 2C). Similarly, representative hummingbird receptive fields from one track are shown in Figure 2D. Across most of its rostrocaudal axis, rWulst was approximately 600 μm in height. In the hummingbird, the rWulst was approximately 400 μm in height. This general conformation of the dorsoventral axis corresponding broadly to the anterior-posterior axis of the body was also found in hindlimb representations.

Across the rWulst's long axis, the non-facial body was also represented modularly, with areas corresponding to neck, breast, wing, foot surface, and tail. In both species, there were many distinct fields corresponding to hindlimb's skin (Figures 2E and 2F). In hummingbirds, foot-related receptive fields accounted for 17.8% of rWulst responses, whereas in finches, these fields accounted for 10.1% of responses.

Responses to naturalistic airborne stimuli

We next investigated whether multiunit responses in rWulst could be elicited from semi-naturalistic air-puff stimuli to mimic aerial contact associated with wind gusts or flight. After identifying the location of a receptive field via manual contact, we positioned an air-puff stimulus 2 cm from its center (Figure 2G). These body areas included the chest and wing, including covert and leading-edge feathers.

Robust bursts of spiking were elicited as each air puff deflected feathers (Figures 2H and 2I). Furthermore, changing the air stimulus angle appeared to modulate response latency and spike density, suggesting a role for directional encoding of gusts or feather position. Systematic measurements of air-puff amplitude and direction are necessary to draw stronger conclusions about the tactile information provided by aerial stimuli.

rWulst response properties

In single unit-recordings, once the general receptive field location was determined using repeated manual tactile stimulation, a piezoelectric stimulator was positioned within the center of the field and single-unit activity was recorded (Figures 2J and 2K). Most responses recorded in both hummingbird (94/123) and finch (187/243) rWulst continued to respond to ongoing indentation of the receptive field (i.e., slow adaptation) for all stimulus lengths (100 ms to 2 s). With increasing stimulus amplitude (from 0.5 mm to 2 mm), neurons increased firing frequency.

Next, we assessed body tactile sensitivity using calibrated von Frey filaments. In hummingbird rWulst, activation thresholds ranged from 8 mN (the lowest calibrated amplitude) to 400 mN, whereas in the finch these measurements varied from 20 mN to 600 mN (Figure 2L). In both species, the lowest activation thresholds were on the hindlimb and tail feathers, whereas the highest threshold corresponded to areas of the back/scapula. In one hummingbird case, we also noted that the wing's leading edge responded to 8 mN deflection.

We measured the surface area of receptive fields on body photographs. For hummingbirds, the smallest fields were on the wing's leading edge (0.008 cm^2) and foot (0.01 to 0.035 cm^2), and the largest (0.58 cm^2 to 3.59 cm^2 ; \bar{x} = 0.96, SEM = 0.021 cm^2) were on the back. Finches demonstrated a

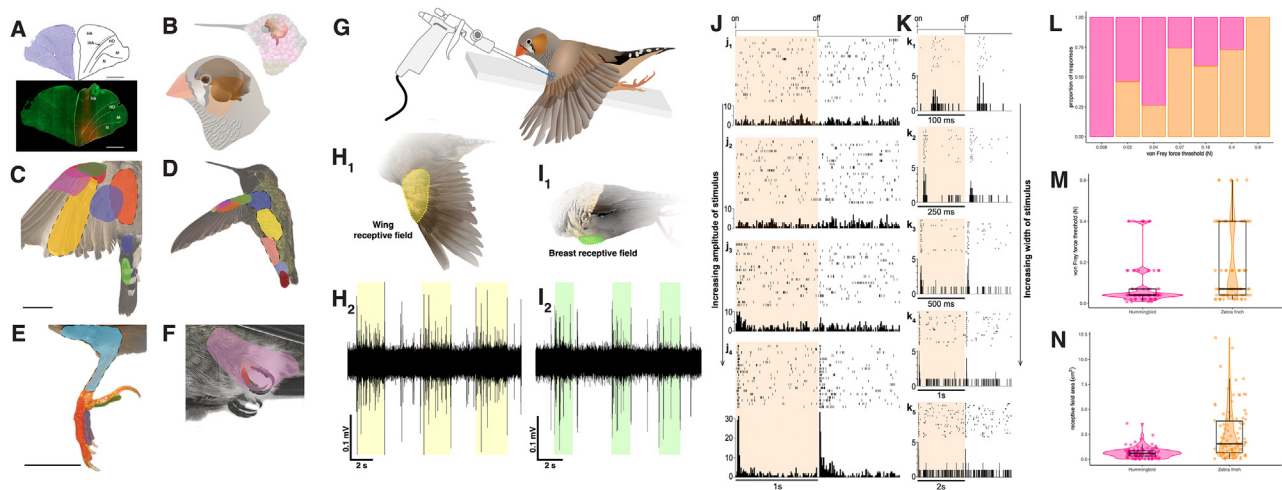


Figure 2. Central organization and response properties of the somatosensory Wulst

(A) Photomicrographs of coronal sections through the hyperpallium. Top: Nissl-stained coronal section (top, left) and anatomical borders (top, right) in the rostral telencephalon of the zebra finch. Scale bar = 1 mm. Bottom: Photomicrograph showing recording site (red) in the rostral Wulst of the finch. Fluorescent Nissl stain (green) used to identify anatomical borders. HA, hyperpallium apicale; IHA, interstitial nucleus of the hyperpallium apicale; HD, hyperpallium densocellulare; M, mesopallium; N, nidopallium. Scale bar = 1 mm.

(B) Illustration showing the orientation of the brain and rostral (somatosensory) Wulst in Anna's hummingbird (top) and zebra finch (bottom).

(C) Example tactile receptive field borders distributed over the wing in the finch within a single electrode track and (D) the hummingbird. Scale = 1 cm.

(E) Example tactile receptive field borders distributed over the hindlimb in finch and (F) the hummingbird. Scale = 1 cm.

(G) Illustration of experimental prep for delivering naturalistic airflow. Small puffs of compressed air (1–2s) were delivered to identified receptive fields while simultaneously recording single units in the rWulst.

(H) Wing receptive field comprised of coverts and alula (H_1) defined by yellow shading. Raw neural trace (H_2) from rWulst corresponding to cell with receptive field shown in H_1 . Yellow highlighted region of trace indicates stimulus “on” period; i.e., air puff is applied to the receptive field during the yellow period. Cell activity is increased during the air-puff stimulus.

(I) Finch breast receptive field defined by green shading (I_1). Raw neural trace from rWulst neuron (I_2) corresponding to receptive field shown in I_1 . Green highlighted region of trace indicates stimulus “on” period; i.e., air puff is applied to the receptive field during the green period. Cell activity is increased during the air-puff stimulus.

(J) Raster plots and peri-stimulus time histograms (PSTH) for finch rostral Wulst neuron in response to computer-controlled piezo-electric mechanical stimulus. Amplitude of stimulus increases from 0.5 mm (j_1) to 2 mm (j_4). Orange panels indicate sustained stimulus “on” period.

(K) Raster plots and PSTH summarizing finch rWulst neuron responses to a computer-controlled piezo-electric mechanical stimulus with increasing length stimulus “on” period. Stimulus period increases from 100 ms (k_1) to 2 s (k_6). Orange panels indicate stimulus “on” period.

(L) Stacked proportional histogram of responding rWulst units and mechanical threshold (von Frey force, N).

(M) Violin plot of receptive field threshold for each species. Hummingbird responses are clustered at lower thresholds than finch responses. For recordings in the rostral Wulst, a Mann-Whitney U test showed that there was a significant difference ($W = 2501.5$; $p < 0.0001$) between von Frey thresholds for hummingbirds ($n = 89$) compared to zebra finches ($n = 94$). The median von Frey threshold was 0.04 N for hummingbirds and 0.07 N for zebra finches. The rank-biserial correlation, as the measure of effect size is -0.4 , indicating a very large effect size according to conventions.³⁵

(N) Violin plot of receptive field area for hummingbird and finch. In comparison to the wide distribution of areas found among finch fields, hummingbird receptive fields are relatively smaller in surface area. For recordings in the rostral Wulst, a Mann-Whitney U test showed that there was a significant difference ($W = 1871$, $p < 0.0001$) between receptive field areas for hummingbirds ($n = 89$) compared to zebra finches ($n = 94$). The median receptive field area was 0.59 cm² for hummingbirds and 1.55 cm² for zebra finches. The rank-biserial correlation, as the measure of effect size is -0.55 , indicating a very large effect size according to conventions.³⁵ Magenta = hummingbird; orange = zebra finch.

similar pattern; smallest receptive fields corresponded to the foot (0.043 cm²–0.16 cm²) and largest to the back (2.18 cm²–12.17 cm²; $\chi = 4.42$, SEM = 2.56).

Examining species-specific sensitivity, we found a higher proportion of hummingbird rWulst sites showed acute sensitivity to mechanical stimuli (i.e., low von Frey force thresholds; Figure 2L). Using a Mann-Whitney U test, we recorded hummingbird rWulst neurons ($n = 89$) had significantly lower von Frey thresholds compared to finches ($n = 94$) (Figure 2M; $W = 2501.5$; $p < 0.0001$; rank-biserial correlation = -0.4). The median von Frey thresholds were 0.04 N and 0.07 N for hummingbirds and finches, respectively.

Hummingbird receptive field areas were primarily clustered in smaller sizes (under 2 cm²) compared to the wider range of areas

in finches (Figure 2N). A Mann-Whitney U test showed that field areas were significantly smaller ($W = 1871$; $p < 0.0001$; rank-biserial correlation = -0.55) in hummingbirds ($n = 89$) compared to finches ($n = 94$). The median field areas were 0.59 cm² and 1.55 cm² in hummingbirds and finches, respectively. The rank-biserial correlation, as the measure of effect size, indicated “very large” effect sizes for species differences in both von Frey threshold and field area.³⁵

Nucleus basorostralis central organization

As the direct target of the trigeminal principal sensory nucleus via the quinfrofrontal tract, the nucleus basorostralis (Bas) is a multimodal nucleus in the avian ventral anterior telencephalon (Figures 3A–3C).^{5,32} Given the variation of body regions

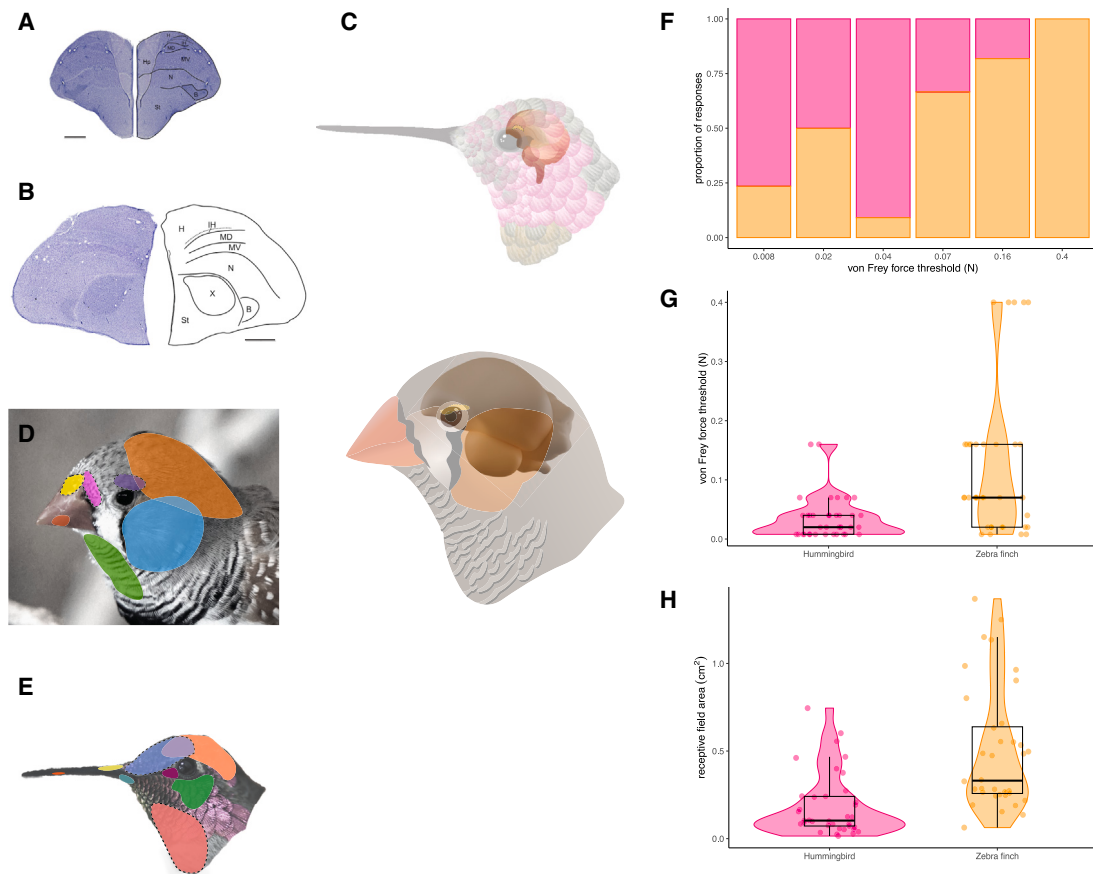


Figure 3. Central organization and response properties of nucleus basorostralis

Photomicrographs of Nissl-stained coronal section and anatomical borders in the rostral telencephalon of the hummingbird (A) and zebra finch (B). H, hyperpallium; IH, intercalated hyperpallium; MD, dorsal mesopallium; MV, ventral mesopallium; N, nidopallium; B, basorostralis; St, striatum; Hp, hippocampus; X, area X. Scale bar = 1 mm.

(C) Illustration showing the orientation of the brain and nucleus basorostralis (Bas) (yellow) in Anna's hummingbird and (bottom) zebra finch.

(D) Example tactile receptive fields distributed over the head and beak in finches and in (E) hummingbirds.

(F) Stacked proportional histogram of responding Bas units and mechanical threshold (von Frey force, N).

(G) Violin plot of receptive field threshold for each species. Hummingbird responses are clustered at lower thresholds than finch responses. For recordings in nucleus Bas, a Mann-Whitney U test showed that there was a significant difference ($W = 331.5$; $p < 0.001$) between von Frey thresholds for hummingbirds ($n = 37$) compared to zebra finches ($n = 36$). The median von Frey threshold was 0.02 N for hummingbirds and 0.07 N for zebra finches. The rank-biserial correlation, as the measure of effect size is -0.5 , indicating a very large effect size according to Funder & Ozer (2019) conventions.

(H) Violin plot of receptive field area for hummingbird and finch. In comparison to the wide distribution of areas found among finch fields, hummingbird receptive fields are relatively smaller in surface area. For recordings in nucleus Bas, a Mann-Whitney U test showed that there was a significant difference ($W = 216.50$; $p < 0.0001$) between receptive field areas for hummingbirds ($n = 37$) compared to zebra finches ($n = 36$). The median receptive field area was 0.1 cm^2 for hummingbirds and 0.33 cm^2 for zebra finches. The rank-biserial correlation, as the measure of effect size is -0.67 , indicating a very large effect size according to conventions.³⁵ Magenta = hummingbird; orange = zebra finch.

represented, from the beak and bill alone in pigeons⁵ and finches⁸ to the entire body surface in barn owls³⁶ and budgerigars,⁷ we wondered to what extent the hummingbird basorostralis might follow either pattern. We hypothesized that hummingbirds might show expanded representation in trigeminal projections encoding beak input. Secondarily, we investigated whether auditory responses neighbored somatosensory representations, similar to those in the budgerigar.⁷

In both species, we found representations were dominated by areas innervated via the trigeminal system. These areas included the caudal portion of the head, areas adjacent to the eyes, and the neck (Figures 3D and 3E) At more anterior

areas of Bas, we identified fields corresponding to the beak, which progressed from proximal to distal as the electrode was moved rostrally. We did not identify any auditory responses despite repeated presentations. Furthermore, all fields within Bas appeared to correspond to the head, neck, and beak, with no distinct responses to post-cranial body surface tactile stimulation.

Nucleus basorostralis response properties

The majority (74%) of neuronal responses (14/19) appeared to be rapidly adapting, with an excitatory response at onset and offset of the 500 ms stimulus. In contrast, 26% of responses (5/19)

appeared to be slowly adapted or tonic, with ongoing spiking during stimulation.

In hummingbird Bas, we found that fields spanning the beak, cheek, chin, and adjacent to the eye had thresholds corresponding to the finest filaments (8 mN), whereas areas corresponding to the head's posterior surface required greater force (70 mN to 160 mN). In finch Bas, we found that 8 mN elicited activity across beak, chin, and throat surfaces, while the head's crown area required the greatest measured indentation (400 mN). A higher proportion of high-sensitivity Bas sites were measured in hummingbirds compared to finches (low von Frey force thresholds; Figure 3F). Using a Mann-Whitney U test, we observed that hummingbird Bas neurons ($n = 37$) had significantly lower von Frey thresholds compared to finches ($n = 36$) (Figure 3G; $W = 331.5$; $p < 0.001$; rank-biserial correlation = -0.5). The median von Frey thresholds were 0.02 N and 0.07 N for hummingbirds and finches, respectively.

Examining Bas receptive field area, the smallest surface areas were recorded across the beak and chin. For example, our smallest receptive field (0.015 cm^2) was found on the hummingbird beak. The largest fields were found on the back surface of the head in both species, with the largest fields corresponding to the finch's crown ($\bar{x} = 0.73$; SEM = 0.44 cm^2) (Figure 3H). A Mann-Whitney U test showed that receptive field areas were significantly smaller ($W = 216.50$; $p < 0.0001$; rank-biserial correlation = -0.67) in hummingbirds ($n = 37$) compared to zebra finches ($n = 36$). The median receptive field area was 0.1 cm^2 and 0.33 cm^2 for hummingbirds and finches, respectively. (Figure 3H). The rank-biserial correlation, as the measure of effect size, indicated "very large" effect sizes for species differences in both von Frey threshold and receptive field area.³⁵

DISCUSSION

Avian somatosensory system representation

Given the diversity of somatotopic arrangements that have been identified among classical models of somatosensation (e.g., rodents),^{37,38} we were interested in exploring whether similar somatotopic maps are present within birds—the most diverse group of land vertebrates, with more than 10,000 extant species.³⁹ One key finding of our study is the identification of clearly defined tactile receptive fields within the avian forebrain. Building from the seminal work of Wild and colleagues, who recorded multiunit responses from rWulst and Bas in songbirds,⁸ owls,^{36,40} and ducks,⁴¹ among others (Figure 4A), we employed single unit analyses, observing robust neuronal responses in specific regions during mechanical stimulation, indicating the presence of dedicated tactile processing circuits. These nuclei were characterized by spatially and anatomically segregated receptive fields, suggesting a topographic representation of tactile information in the avian forebrain (Figures 4B and 4C). Specifically, we found that areas corresponding to the head, neck, and beak were robustly represented within Bas. In both hummingbird (Video S1) and finch (Video S2), these representations followed a generalized pattern. Receptive fields corresponding to dorsal regions (e.g., the maxillary beak) were typically found superior to ventral regions (e.g., the mandibular beak). Our recording preparation precluded detailed mapping of intraoral regions or the tongue, an area that deserves further detailed investigation.

Like the arrangement noted in pigeons,^{3,4} rWulst of both hummingbirds and finches encompassed areas exclusively corresponding to the post-cranial body. Along its rostrocaudal axis, rWulst featured receptive fields related to the breast, wing, back, and tail feathers, respectively. Following this same rWulst axis in both species, we also encountered large areas dedicated to tactile responses from the glabrous foot surface and adjacent feathers. This was positioned directly adjacent to areas corresponding to the back and tail feathers. This distinct rWulst organization of the hindlimb surface and associated regions is reminiscent of the prominent claw representation found in the barn owl rWulst,⁴⁰ a species which notably employs its talons in securing prey. While hummingbirds and finches do not immobilize prey using their feet, these sensory surfaces are used in a variety of important tactile tasks. These include spending significant time perched, with their feet well-adapted for gripping branches, nest building, preening, and scratching. Finches also routinely use their feet while feeding, holding vegetation or seeds for manipulation with the beak. Further examination of the proportional volume of body representation within rWulst could shed light on whether this notable hindlimb representation shows similarities to the enhanced representation of discrete body surfaces, as observed primarily in mammalian primary somatosensory cortex. This phenomenon of "cortical magnification"—the preferential allocation of cortical real estate to behaviorally significant sensory receptors, such as hands and lips in primates⁴⁶—is thought to contribute to increased sensory resolution for important areas of the body periphery. As this appears to be the case in the barn owl (to the extent that the body is no longer represented within the rWulst), further physiological research employing other birds that use their hindlimbs for complex manipulations (e.g., falcons, hawks, and parrots⁴⁷), could shed light on detailed representation of the foot surface. Physiological and anatomical examinations of the Bas in the dunlin (probe-feeding specialist)⁴⁵ suggest that preferential expansion in representation of important tactile surfaces (e.g., the bill tip) might be found among other birds.

Receptive field properties

Avian mechanotransduction differs from mammalian systems in several fundamental ways.⁴⁸ Forebrain somatosensation is processed in the hyperpallium and discrete nidopallial nuclei, ventral to the superficial pallium, whereas primary somatosensory cortex (S1) is distributed across the laminated neocortex. At the periphery, mammals rely upon diverse classes of mechanoreceptor end organs (e.g., Pacinian and Meissner corpuscles and Merkel complexes) and tactile organs associated with the follicle complex of specialized vibrissae. Although birds also have some classes of homologous mechanoreceptor end organs (e.g., Herbst and Grandry corpuscles), most of their bodies are covered by distinct populations of diverse feather types. Therefore, we wondered how basic receptive field properties including area and mechanical thresholds might compare to classically studied somatosensory models.

In general terms, smaller receptive fields are associated with higher sensitivity. Smaller receptive fields allow for greater spatial resolution. For example, human fingertips and lips have

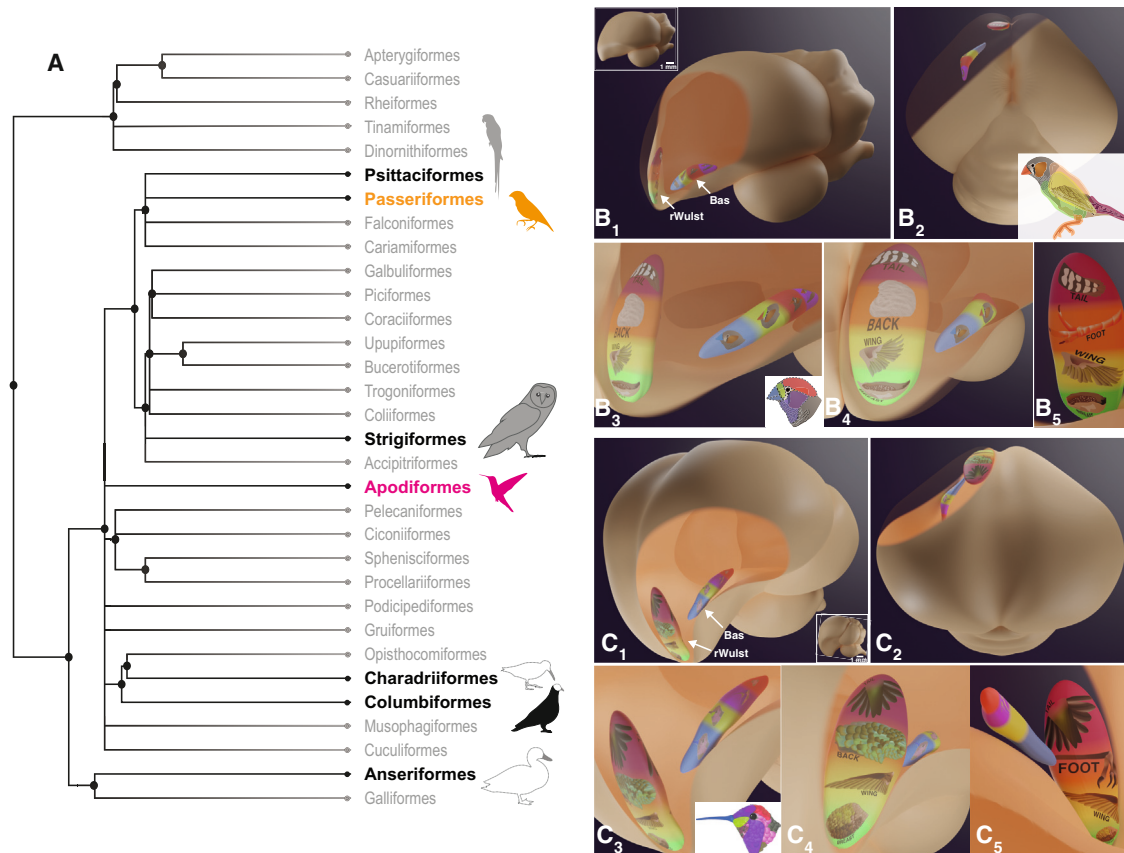


Figure 4. Comparative view of the avian somatosensory system representation

(A) Illustration of phylogenetic relationships between avian orders. Black text indicates groups for which somatosensory data from the rostral Wulst or nucleus basorostralis has been reported. Animal illustrations provide a general indication of which body parts are represented in each nucleus (gray fill, basorostralis; black fill, rostral Wulst); e.g., budgerigars (Psittaciformes)⁷ have representations of the body and beak in basorostralis, barn owls (Strigiformes) have a representation of the claw in the rWulst^{39,42} and representation of the body and beak in basorostralis, while pigeons (Columbiformes) have a beakless representation in the rostral Wulst⁴ and the beak is represented in basorostralis.^{6,43,44} In anseriformes³ and charadriiformes,⁴⁵ the beak is represented in basorostralis. Groups used in the present study are highlighted in orange (zebra finches) and magenta (hummingbirds).

(B) 3D illustrations of the zebra finch brain with interior views showing relative size and position of rostral Wulst (rWulst) and basorostralis (Bas) in the left hemisphere. Color indicates region of body represented. For rWulst: magenta, tail; anterior light orange, back; posterior dark orange, foot; yellow, wing; and green, breast. For Bas: blue, beak; yellow-green, near beak; red, crown; and purple, cheek, chin, and throat. (B₁) Sagittal view of the finch brain, rostral pole to the left, caudal pole to the right. Inset shows a sagittal view of the brain with no opacity so that gross anatomy can be visualized. (B₂) Dorsal view of finch brain. The inset shows the colour scheme of the neural somatotopy using a finch illustration. The colour scheme is the same for the hummingbird rWulst (B₃) Magnified view of the rostral telencephalon illustrating body representation in the rWulst and beak and head representation in Bas. Note that both color and drawings of the body/head region indicate the area represented in each nucleus. The inset shows how regions of the head are represented in Bas. (B₄) Magnified view of rostral telencephalon; more anterior view than B₃. (B₅) Caudal view of rWulst. Image acquired from inside the brain looking anteriorly. Note, from this angle, the foot representation is visible.

(C) 3D illustrations of the hummingbird brain with interior views showing relative size and position of rWulst and Bas in the left hemisphere. Color indicates region of body represented. For rWulst: magenta, tail; anterior orange, back; posterior orange, foot; yellow, wing; and green, breast. For Bas: blue, beak; yellow-green, near beak and chin; red, crown; and purple, cheek, throat, and near eye. (C₁) ³/₄ view of the hummingbird brain with relative position of rWulst and Bas visible. Inset shows a sagittal view of the hummingbird brain with no opacity so that gross anatomy can be visualized. Rostral pole is to the left, caudal pole to the right. (C₂) Dorsal view of hummingbird brain. Note that the brain model has been pitched backwards to give a clear view of rWulst and Bas. (C₃) Magnified view of the rostral telencephalon illustrating the body representation in rWulst and beak and head representation in Bas. Note that both color and drawings of the body/head region indicate the area represented in each nucleus. The inset shows how regions of the head are represented in Bas. (C₄) Magnified view of the rostral telencephalon; more anterior view than C₃. (C₅) Caudal view of rWulst. Image acquired from inside the brain looking anteriorly. Note that, from this angle, the foot representation is visible. See also [Videos S1](#) and [S2](#).

minute receptive fields and a high density of touch receptors, providing peripheral adaptations for acute tactile sensitivity and precision.⁴⁹

Conversely, larger receptive fields are typically associated with lower sensitivity. Areas including the back or upper

hindlimbs have larger receptive fields and fewer mechanoreceptors, resulting in lower tactile sensitivity and spatial resolution. This inverse relationship between receptive field area and mechanical thresholds has been explored in other vertebrates, including in close avian relatives, the archosaurs.⁵⁰ Given the

prominent talon representation in both owl Bas³⁹ and the foot in rWulst in hummingbirds and finches, combined with recent insight into the diversity of foot usage among diverse bird lineages,⁴⁷ broader investigation of avian hindlimb tactile specialization and its telencephalic representation could yield insight into general principles of sensory adaptation.

Our study focused primarily on the avian forebrain, and further analyses are warranted to explore tactile processing in other avian brain regions, including the brainstem and diencephalon. Prior investigations using extracellular radial nerve recordings, corresponding to mechanical and air puff stimuli in chickens, suggest that feathers can respond robustly to airflow stimuli of varying directions.⁵¹ Further neurophysiological recordings along the somatosensory neuroaxis might reveal segregation in processing differing somatosensory input (e.g., pain vs. mechanical deflection), similar to segregation of trigeminal brainstem relays in mammals.⁵² Additionally, future studies could employ more advanced techniques, such as *in vivo* imaging, to gain a more comprehensive understanding of the neural dynamics and circuitry underlying avian tactile processing. Molecular techniques have identified ion channel contributions to tactile and thermal sensation, exploiting the abundance of sensory end organs within the duck beak.⁵³ Similar approaches applied comparatively across avian taxa⁵⁴ may further illuminate diversity in sensory ion channel function and the evolutionary interplay between sensory structures, neural processing, and behavioral adaptation.

In conclusion, our investigation provides novel insights into tactile receptive field organization and response properties in the avian forebrain, using hummingbirds and finches, which vary in their tactile behavior and ecology. By delineating architectural principles and functional properties of avian tactile processing in the hyperpallium and basorostralis, we contribute to the broader field of comparative neurobiology and enhance our understanding of sensory systems. Future research in this area may unveil further intricacies of avian tactile perception and shed light on the remarkable sensory capabilities of birds.

STAR★METHODS

Detailed methods are provided in the online version of this paper and include the following:

- KEY RESOURCES TABLE
- RESOURCES AVAILABILITY
 - Lead contact
 - Materials availability
 - Data and code availability
- EXPERIMENTAL MODEL AND SUBJECT DETAILS
- METHOD DETAILS
 - *In vivo* labeling
 - Electrophysiological measurements
 - Sensory stimuli
- QUANTIFICATION AND STATISTICAL ANALYSIS
 - Data collection and analysis
 - Receptive field quantification
 - Hypothesis testing

SUPPLEMENTAL INFORMATION

Supplemental information can be found online at <https://doi.org/10.1016/j.cub.2024.04.081>.

ACKNOWLEDGMENTS

A.H.G. was supported by funding from The Royal Society (RGS\R2\212436). D.B.L. was supported by Natural Sciences and Engineering Research Council of Canada RGPIN-2021-03180, DGEGR-2021-00130, and funding from Integrative Biology and Physiology (UCLA). We thank Dr. Melissa Armstrong and members of the Doug Altshuler lab for generosity in technical preparations and discussion. We also thank Robert Shadwick, Bill Milsom, and Benjamin Matthews (University of British Columbia, Comparative Physiology cluster in Zoology) for their technical support and advice.

AUTHOR CONTRIBUTIONS

A.H.G. and D.B.L. conceived the study. A.H.G. and D.B.L. collected the data. A.H.G., D.B.L., and P.-H.W. analyzed the data. A.H.G. and D.B.L. wrote and edited the manuscript.

DECLARATION OF INTERESTS

The authors declare no competing interests.

Received: October 24, 2023

Revised: March 25, 2024

Accepted: April 30, 2024

Published: May 29, 2024

REFERENCES

1. Woolsey, T.A., and Van der Loos, H. (1970). The structural organization of layer IV in the somatosensory region (SI) of mouse cerebral cortex: the description of a cortical field composed of discrete cytoarchitectonic units. *Brain Res.* 17, 205–242.
2. Petersen, C.C.H. (2007). The functional organization of the barrel cortex. *Neuron* 56, 339–355. <https://doi.org/10.1016/j.neuron.2007.09.017>.
3. Funke, K. (1989). Somatosensory areas in the telencephalon of the pigeon: I. Response characteristics. *Exp. Brain Res.* 76, 603–619.
4. Wild, J.M. (1987). The avian somatosensory system: connections of regions of body representation in the forebrain of the pigeon. *Brain Res.* 412, 205–223.
5. Wild, J.M., Arends, J.J., and Zeigler, H.P. (1985). Telencephalic connections of the trigeminal system in the pigeon (*Columba livia*): a trigeminal sensorimotor circuit. *J. Comp. Neurol.* 234, 441–464.
6. Witkovsky, P., Zeigler, H.P., and Silver, R. (1973). The nucleus basalis of the pigeon: A single-unit analysis. *J. Comp. Neurol.* 147, 119–128.
7. Wild, J.M., Reinke, H., and Farabaugh, S.M. (1997). A non-thalamic pathway contributes to a whole body map in the brain of the budgerigar. *Brain Res.* 755, 137–141.
8. Wild, J.M., and Farabaugh, S.M. (1996). Organization of afferent and efferent projections of the nucleus basalis prosencephali in a passerine, *Taeniopygia guttata*. *J. Comp. Neurol.* 365, 306–328.
9. Rico-Guevara, A., and Rubega, M.A. (2011). The hummingbird tongue is a fluid trap, not a capillary tube. *Proc. Natl. Acad. Sci. USA* 108, 9356–9360.
10. Ewald, P.W., and Williams, W.A. (1982). Function of the bill and tongue in nectar uptake by hummingbirds. *The Auk* 99, 573–576.
11. Gaede, A.H., Baliga, V.B., Smyth, G., Gutiérrez-Ibáñez, C., Altshuler, D.L., and Wylie, D.R. (2022). Response properties of optic flow neurons in the accessory optic system of hummingbirds versus zebra finches and pigeons. *J. Neurophysiol.* 127, 130–144.
12. Gaede, A.H., Goller, B., Lam, J.P.M., Wylie, D.R., and Altshuler, D.L. (2017). Neurons responsive to global visual motion have unique tuning properties in hummingbirds. *Curr. Biol.* 27, 279–285.
13. Smyth, G., Baliga, V.B., Gaede, A.H., Wylie, D.R., and Altshuler, D.L. (2022). Specializations in optic flow encoding in the pretectum of hummingbirds and zebra finches. *Curr. Biol.* 32, 2772–2779.e4.

14. Watanabe, I., Usukura, J., and Yamada, E. (1985). Electron microscope study of the Grandry and Herbst corpuscles in the palatine mucosa, gingival mucosa and beak skin of the duck. *Arch. Histol. Jpn.* **48**, 89–108.
15. Cunningham, S.J., Corfield, J.R., Iwaniuk, A.N., Castro, I., Alley, M.R., Birkhead, T.R., and Parsons, S. (2013). The anatomy of the bill tip of kiwi and associated somatosensory regions of the brain: comparisons with shorebirds. *PLoS One* **8**, e80036.
16. Cunningham, S.J., Alley, M.R., Castro, I., Potter, M.A., Cunningham, M., and Pyne, M.J. (2010). Bill morphology of ibises suggests a remote-tactile sensory system for prey detection. *The Auk* **127**, 308–316.
17. du Toit, C.J., Chinsamy, A., and Cunningham, S.J. (2022). Comparative morphology and soft tissue histology of the remote-touch bill-tip organ in three ibis species of differing foraging ecology. *J. Anat.* **241**, 966–980.
18. Delaunay, M.G., Brasseur, C., Larsen, C., Lloyd, H., and Grant, R.A. (2022). The evolutionary origin of avian facial bristles and the likely role of rictal bristles in feeding ecology. *Sci. Rep.* **12**, 21108.
19. Cunningham, S.J., Alley, M.R., and Castro, I. (2011). Facial bristle feather histology and morphology in New Zealand birds: implications for function. *J. Morphol.* **272**, 118–128.
20. Delaunay, M.G., Charter, M., and Grant, R.A. (2022). Anatomy of bristles on the nares and rictus of western barn owls (*Tyto alba*). *J. Anat.* **241**, 527–534.
21. Yu, M., Yue, Z., Wu, P., Wu, D.-Y., Mayer, J.-A., Medina, M., Wideltz, R.B., Jiang, T.-X., and Chuong, C.-M. (2004). The developmental biology of feather follicles. *Int. J. Dev. Biol.* **48**, 181–191.
22. Crole, M.R., and Soley, J.T. (2014). Comparative distribution and arrangement of Herbst corpuscles in the oropharynx of the ostrich (*Struthio camelus*) and emu (*Dromaius novaehollandiae*). *Anat. Rec.* **297**, 1338–1348. <https://doi.org/10.1002/ar.22933>.
23. Weir, K.A., and Lunam, C.A. (2004). A histological study of emu (*Dromaius novaehollandiae*) skin. *J. Zool.* **264**, 259–266.
24. Hörster, W. (1990). Histological and electrophysiological investigations on the vibration-sensitive receptors (Herbst corpuscles) in the wing of the pigeon (*Columba livia*). *J. Comp. Physiol.* **166**, 663–673.
25. Halata, Z., and Munger, B.L. (1980). The ultrastructure of Ruffini and Herbst corpuscles in the articular capsule of domestic pigeon. *Anat. Rec.* **198**, 681–692.
26. Berkhoudt, H. (1979). The morphology and distribution of cutaneous mechanoreceptors (Herbst and Grandry corpuscles) in bill and tongue of the mallard (*Anas platyrhynchos* L.). *Neth. J. Zool.* **30**, 1–34.
27. Winkelmann, R., and MYERS, T.T., 3rd. (1961). The histochemistry and morphology of the cutaneous sensory end-organs of the chicken. *J. Comp. Neurol.* **117**, 27–35.
28. Zelená, J., Halata, Z., Szeder, V., and Grim, M. (1997). Crural Herbst corpuscles in chicken and quail: numbers and structure. *Anat. Embryol.* **196**, 323–333.
29. Cunningham, S.J., Alley, M.R., and Castro, I. (2011). Facial bristle feather histology and morphology in New Zealand birds: implications for function. *J. Morphol.* **272**, 118–128.
30. Necker, R. (1989). Cells of origin of spinothalamic, spinotectal, spinoreticular and spinocerebellar pathways in the pigeon as studied by the retrograde transport of horseradish peroxidase. *J. Hirnforsch.* **30**, 33–43.
31. Frost, B., Wylie, D., and Wang, Y. (1994). The analysis of motion in the visual systems of birds. *Perception and motor control in birds: An ecological approach*, pp. 248–269.
32. Wild, J.M. (2022). Chapter 9 - The avian somatosensory system: a comparative view. In *Sturkie's Avian Physiology, Seventh Edition*, C.G. Scanes, and S. Dridi, eds. (Academic Press), pp. 123–137. <https://doi.org/10.1016/B978-0-12-819770-7.00018-9>.
33. Wild, J.M., and Williams, M.N. (2000). Rostral wulst in passerine birds. I. Origin, course, and terminations of an avian pyramidal tract. *J. Comp. Neurol.* **416**, 429–450.
34. Jarvis, E.D., Yu, J., Rivas, M.V., Horita, H., Feenders, G., Whitney, O., Jarvis, S.C., Jarvis, E.R., Kubikova, L., Puck, A.E.P., et al. (2013). Global view of the functional molecular organization of the avian cerebrum: mirror images and functional columns. *J. Comp. Neurol.* **521**, 3614–3665. <https://doi.org/10.1002/cne.23404>.
35. Funder, D.C., and Ozer, D.J. (2019). Evaluating effect size in psychological research: Sense and nonsense. *Advances in methods and practices in psychological science* **2**, 156–168.
36. Wild, J.M., Kubke, M.F., and Carr, C.E. (2001). Tonotopic and somatotopic representation in the nucleus basalis of the barn owl, *Tyto alba*. *Brain Behav. Evol.* **57**, 39–62. <https://doi.org/10.1159/000047225>.
37. Delmas, P., Hao, J., and Rodat-Despoix, L. (2011). Molecular mechanisms of mechanotransduction in mammalian sensory neurons. *Nat. Rev. Neurosci.* **12**, 139–153. <https://doi.org/10.1038/nrn2993>.
38. Inan, M., and Crair, M.C. (2007). Development of cortical maps: perspectives from the barrel cortex. *Neuroscientist* **13**, 49–61.
39. Brusatte, S.L., O'Connor, J.K., and Jarvis, E.D. (2015). The Origin and Diversification of Birds. *Curr. Biol.* **25**, R888–R898. <https://doi.org/10.1016/j.cub.2015.08.003>.
40. Wild, J.M., Kubke, M.F., and Peña, J.L. (2008). A pathway for predation in the brain of the barn owl (*Tyto alba*): projections of the gracile nucleus to the "claw area" of the rostral wulst via the dorsal thalamus. *J. Comp. Neurol.* **509**, 156–166. <https://doi.org/10.1002/cne.21731>.
41. Berkhoudt, H., Dubbeldam, J.L., and Zeilstra, S. (1981). Studies on the somatotopy of the trigeminal system in the mallard, *Anas platyrhynchos* L. IV. Tactile representation in the nucleus basalis. *J. Comp. Neurol.* **196**, 407–420. <https://doi.org/10.1002/cne.901960305>.
42. Manger, P.R., Elston, G.N., and Pettigrew, J.D. (2002). Multiple maps and activity-dependent representational plasticity in the anterior Wulst of the adult barn owl (*Tyto alba*). *Eur. J. Neurosci.* **16**, 743–750. <https://doi.org/10.1046/j.1460-9568.2002.02119.x>.
43. Wild, J.M. (1997). The avian somatosensory system: the pathway from wing to Wulst in a passerine (*Chloris chloris*). *Brain Res.* **759**, 122–134. [https://doi.org/10.1016/S0006-8993\(97\)00253-9](https://doi.org/10.1016/S0006-8993(97)00253-9).
44. Dubbeldam, J.L., Brauch, C.S., and Don, A. (1981). Studies on the somatotopy of the trigeminal system in the mallard, *Anas platyrhynchos* L. III. Afferents and organization of the nucleus basalis. *J. Comp. Neurol.* **196**, 391–405. <https://doi.org/10.1002/cne.901960304>.
45. Pettigrew, J.D., and Frost, B.J. (1985). A tactile fovea in the *Scolopacidae*? *Brain Behav. Evol.* **26**, 105–195.
46. Sur, M., Merzenich, M.M., and Kaas, J.H. (1980). Magnification, receptive-field area, and "hypercolumn" size in areas 3b and 1 of somatosensory cortex in owl monkeys. *J. Neurophysiol.* **44**, 295–311.
47. Gutiérrez-Ibáñez, C., Amaral-Peçanha, C., Iwaniuk, A.N., Wylie, D.R., and Baron, J. (2023). Online repositories of photographs and videos provide insights into the evolution of skilled hindlimb movements in birds. *Commun. Biol.* **6**, 781. <https://doi.org/10.1038/s42003-023-05151-z>.
48. Wullimann, M.F. (2016). Nervous System Architecture in Vertebrates. In *The Wiley Handbook of Evolutionary Neuroscience*, pp. 236–278. <https://doi.org/10.1002/9781118316757.ch9>.
49. Johansson, R.S. (1978). Tactile sensibility in the human hand: receptive field characteristics of mechanoreceptive units in the glabrous skin area. *J. Physiol.* **281**, 101–125. <https://doi.org/10.1113/jphysiol.1978.sp012411>.
50. Leitch, D.B., and Catania, K.C. (2012). Structure, innervation and response properties of integumentary sensory organs in crocodylians. *J. Exp. Biol.* **215**, 4217–4230. <https://doi.org/10.1242/jeb.076836>.
51. Brown, R.E., and Fedde, M.R. (1993). Airflow Sensors in the Avian Wing. *J. Exp. Biol.* **179**, 13–30. <https://doi.org/10.1242/jeb.179.1.13>.
52. Ren, K., and Dubner, R. (2011). The role of trigeminal interpolaris-caudalis transition zone in persistent orofacial pain. *Int. Rev. Neurobiol.* **97**, 207–225. <https://doi.org/10.1016/B978-0-12-385198-7.00008-4>.
53. Schneider, E.R., Anderson, E.O., Mastrotto, M., Matson, J.D., Schulz, V.P., Gallagher, P.G., LaMotte, R.H., Gracheva, E.O., and Bagriantsev, S.N. (2017). Molecular basis of tactile specialization in the duck bill.

- Proc. Natl. Acad. Sci. USA *114*, 13036–13041. <https://doi.org/10.1073/pnas.1708793114>.
54. Schneider, E.R., Anderson, E.O., Feketa, V.V., Mastrotto, M., Nikolaev, Y.A., Gracheva, E.O., and Bagriantsev, S.N. (2019). A Cross-Species Analysis Reveals a General Role for Piezo2 in Mechanosensory Specialization of Trigeminal Ganglia from Tactile Specialist Birds. *Cell Rep.* *26*, 1979–1987.e3. <https://doi.org/10.1016/j.celrep.2019.01.100>.
55. Schindelin, J., Arganda-Carreras, I., Frise, E., Kaynig, V., Longair, M., Pietzsch, T., Preibisch, S., Rueden, C., Saalfeld, S., Schmid, B., et al. (2012). Fiji: an open-source platform for biological-image analysis. *Nat. Methods* *9*, 676–682. <https://doi.org/10.1038/nmeth.2019>.

STAR★METHODS

KEY RESOURCES TABLE

REAGENT or RESOURCE	SOURCE	IDENTIFIER
Chemicals, peptides, and recombinant proteins		
Dextran Texas Red 3000 MW	Thermo Fisher Scientific, Ontario, Canada	D3328
Dextran micro-emerald 3000 MW	Thermo Fisher Scientific, Ontario, Canada	D3306
Dil (1, 1'-dioctadecyl-3,3,3'-tetramethylindocarbocyanine)	Invitrogen, Carlsbad, CA, USA	
AM1-43 (styryl dye)	Biotium	
NeuroTrace 500/525	Thermo Fisher Scientific, Ontario, Canada	
thionin	MilliporeSigma	
Ketamine	cdmv	
Xylazine	UBC Animal Care Services	
Deposited data		
Data for manuscript	Figshare	https://doi.org/10.6084/m9.figshare.25606005
Experimental models: Organisms/strains		
Anna's hummingbird (<i>Calypte anna</i>), adult male	Wild caught	N/A
Zebra finch (<i>Taeniopygia gutatta</i>), adult male	L'Oisellerie de l'Estrie, Quebec, Canada	N/A
Software and algorithms		
Spike2 v10	CED, Cambridge, UK	
R v4.3.2	R Core Team	
RStudio v 2023.12.1 + 402	Posit	
ImageJ Fiji		https://doi.org/10.1038/nmeth.2019
Other		
sliding microtome	Leica, Ontario, Canada	
Zeiss AxioImager M2	Zeiss, Jena, Germany	
Von Frey hairs	Stoelting, IL, USA	
Piezo actuator and servo controller	Physik Instrument LP, Auburn, MA, USA	
Stereotaxic frame	David Kopf Instruments, CA, USA	

RESOURCES AVAILABILITY

Lead contact

Further information and requests for resources should be directed to and will be fulfilled by the Lead contact, Duncan Leitch (dleitch@ucla.edu).

Materials availability

This study did not generate new unique reagents.

Data and code availability

- Data reported in this paper will be shared by the [lead contact](#) upon request.
- This paper does not report original code.
- Data are published online at <https://doi.org/10.6084/m9.figshare.25606005>. Any additional information required to reanalyze the data reported in this paper is available from the [lead contact](#) upon request.

EXPERIMENTAL MODEL AND SUBJECT DETAILS

Electrophysiological recordings and histological images were acquired from six adult male Anna's hummingbirds (*Calypte anna*) and 20 adult male zebra finches (*Taeniopygia guttata*). All animal procedures were approved by the University of British Columbia Animal Care Committee in accordance with the guidelines set out by the Canadian Council on Animal Care or conducted according to Home Office guidelines under the UK Animals in Scientific Procedures Act 1986.

METHOD DETAILS

In vivo labeling

Feather-covered hummingbird skin samples were removed postmortem from paraformaldehyde (PFA)-fixed tissues. Small crystals of Dil (1, 1'-dioctadecyl-3,3,3'-tetramethylindocarbocyanine, Invitrogen, Carlsbad, CA) were applied via insect pins to distal branches of spinal nerves innervating the wings, as dissected from the brachial plexus. These samples were embedded in 2% agarose, immersed in 4% PFA, and stored in darkness at 27°C for at least 4 weeks.

In other hummingbirds, AM1-43 (Biotium, Fremont, CA) was diluted in sterile PBS and injected subcutaneously near the convergence of the wing and back. At 22 h post-injection, the wing feathers were manually stimulated via periodic brushing for 1 h. All specimens were sectioned sagittally at 80 μm thickness on a sliding microtome (Leica, Concord, Ontario, Canada) and imaged on a Zeiss Axiomager M2 (Zeiss, Jena, Germany).

Electrophysiological measurements

Stereotaxic surgery was performed using an adapted frame (David Kopf) that secured the head of the hummingbird or zebra finch. Coordinates were derived from Nissl-stained sections and from neuroanatomical measurements in zebra finch basorostralis⁸ and rostral Wulst.⁴ Birds were anesthetized with an intramuscular injection of ketamine/xylazine (65 mg/kg ketamine, 16.7 mg/kg xylazine, i.m.) and supplemental injections to maintain a surgical plane were given as needed. Digital photographs were made of the body surface of each bird to serve as reference for distinguishing boundaries of receptive fields. Initially, the head was angled downward at 45° to the horizontal plane to access the contralateral anterior telencephalon via small craniotomy (approximately 1.5 mm × 1.5 mm), and the dura mater was removed.

Single and multi-unit neuronal recordings were performed using glass microelectrodes (5 μm diameter tip), filled with 2M NaCl, or via 20 MOhm tungsten electrodes (FHC, Bowdoin, ME). A silver wire clipped to the skin adjacent to the incision served as a reference electrode. The recording electrode was attached to a micro manipulator (Sutter, Novato, CA), oriented perpendicularly to the surface of the telencephalon, and advanced while listening to audio output of neural activity in response to gentle mechanical stimuli. Extracellular signals were amplified and filtered (A-M Systems Model 3000) prior to digitization (Cambridge Electronic Design; Power 1401-3).

The locations of recording sites were confirmed via dextran microinjection (Texas Red 3000 MW or micro-Emerald 3000 MW, Thermo Fisher Scientific, Ontario, Canada). After recording, we retracted the recording pipette and removed the saline solution (or switched to a glass electrode if performing recordings with a tungsten electrode), broke the tip to ~20–30 μm diameter tip and refilled the micropipette with a fluorescent conjugated dextran (10% in 10 mM PBS; Texas Red 3000 MW or micro-Emerald 3000 MW, Thermo Fisher Scientific, Ontario, Canada). Then we lowered the micropipette to the recording site and injected the dextran via iontophoresis (±4.5 μA; 7s on/7s off) for 15–40 min. At the end of each experiment, the bird was euthanized via overdose of ketamine/xylazine and transcardially perfused with 0.9% saline followed by 4% PFA. Brains were dissected, cryo-protected in 30% sucrose for at least 3 days, and sectioned (40 μm) coronally. Tissue sections were stained for Nissl substance (NeuroTrace 500/525, incubation time = 20 min, ThermoFisher; thionin, MilliporeSigma) to visualize forebrain architecture, and the location of the dextran injection was verified using a Zeiss Axiomager M2 (Zeiss Research Microscopy, Jena, Germany).

Sensory stimuli

We recorded multi-unit neural responses in response to manual gentle brushing and tapping with wooden probes to investigate the boundaries of tactile receptive fields. First, we gently brushed or stroked the body surface with a wooden applicator with a cotton tip. This stimulus was applied in a repetitive manner, brushing irrespective of direction. Following >30 brushing movements and detailed exploration of the boundaries between responsive and adjacent non-responsive areas, we outline the surface area of the receptive field on scaled photographs of the body surface. Next, upon recording a robust (>50% increase in firing frequency) response, we used the piezoelectric stimulus to apply square pulses, varying in amplitude and frequency. Then we assessed mechanical threshold using calibrated filaments (von Frey hairs, Stoelting, IL) while monitoring spike activity, repeating stimulation with filaments of decreasing force until robust responses were no longer elicited. These receptive fields were manually outlined on digital photographs of the body surface of each bird.

Upon recording from a well isolated unit, a square wave stimulator (Powerlab, AD Instruments, Sydney, Australia) was used drive a preloaded piezo actuator (P-841.20) attached to a E-625 Piezo Servo Controller (Physik Instrument LP, Auburn, MA) which was positioned in the center of the tactile receptive field. The amplitude and length of the square pulse were independently adjusted.

In a second cohort of finches, we also used airflow stimuli, using a custom-built compressor system. After identifying and mapping each receptive field as described above, the airstream was positioned perpendicular to the receptive field, approximately 2 cm from

the surface, and short (1-2s) air bursts were applied. Subsequent trials applied air flow at a range of angles (e.g., simulating forward flight or a wind gust from behind).

We also used auditory stimuli to investigate potential responses. These included a variety of tuning forks of different frequencies, tone generators (Tone Gen Pro, iOS), and digital white noise stimulation from loudspeakers.

QUANTIFICATION AND STATISTICAL ANALYSIS

Data collection and analysis

Neural activity was amplified (x10,000) (A-M Systems, Sequim, WA), bandpass filtered (0.1 to 3 kHz), and acquired at 20 kHz using a CED micro1401-3 (Cambridge, UK). We processed raw neural recordings offline using the spike sorting algorithm in Spike2 (Cambridge Electronic Design, Cambridge, UK) to extract single units. This program enabled us to set trigger thresholds and dimensions of a sliding window encompassing the full spike amplitude to identify individual spikes. These spikes were then matched to full wave templates for classification. We grouped similar templates post-hoc using principal component analysis and visual inspection of overlaid spikes coded by template. Spike sorted data were used to produce raster plots and peri-stimulus time histograms to visualize neural responses to tactile stimuli.

Receptive field quantification

Prior to physiological recordings, we collected digital photographs of the body surface of each hummingbird or finch with a surgical scale bar. Post-surgery, we outlined the borders of drawn receptive fields, calibrated to the scale bar using Fiji software, to measure surface area.⁵⁴

Hypothesis testing

Statistical analyses were performed using R (v4.3.2). Details of statistical tests, including sample sizes and *p* values, are provided in the main text and figure legends. For hypothesis testing, we asked whether mean values of receptive field area and sensitivity were different between species. Data were not normally distributed, so we used a Mann-Whitney U test to test whether sample means were equal or not. We determined effect size (R package “effectsize” v0.8.6) in accordance with rules set by Funder & Ozer (2019), which apply to positive or negative *r* alike and define a “very large” effect as $r \geq 0.4$.⁵⁵